Preparation of partial-thickness burn wounds in rodents using a new experimental burning device

AUTHOR(S):

Sakamoto, Michiharu; Morimoto, Naoki; Ogino, Shuichi; Jinno, Chizuru; Kawaguchi, Atsushi; Kawai, Katsuya; Suzuki, Shigehiko

CITATION:

Sakamoto, Michiharu ...[et al]. Preparation of partial-thickness burn wounds in rodents using a new experimental burning device. Annals of Plastic Surgery 2016, 76: 652-658

ISSUE DATE:

2016-01-01

URL:

http://hdl.handle.net/2433/262405

ABSTRACT

Objective: The manual application of hot water or hot metal to an animal's skin surface is often used to prepare burn wound models. However, manual burn creation is subject to human variability. We developed a new device that can control the temperature, time and pressure of contact to produce precise and reproducible animal burn wounds and investigated the conditions required to prepare various burn wounds using our new device.

Methods: We prepared burn wounds on F344 rats using three contact times 2, 4 and 10 s using a stamp heated to 80°C. We observed the wound-healing process macroscopically and histologically, and evaluated the burn depth using a laser speckle contrast-imaging device, which evaluated the blood flow of the wound.

Results: The changes in the burned area over time, tissue perfusion of the burn wounds, histological evaluation of the burn depth by hematoxylin-eosin and AZAN staining, and the epithelialization rate (the ratio of the epithelialized area to the wound length) were evaluated on histological sections. Results indicated that the burn wounds prepared with contact times of 2, 4 and 10 s corresponded to superficial dermal burns, deep dermal burns

and full-thickness burns, respectively.

Conclusion: We demonstrated that partial- and full-thickness burn wounds can be precisely and reproducibly created with our new automated burning device.

Keywords

Burn model, burn depth, laser speckle contrast imaging (FLPI), burning device, burn depth evaluation

INTRODUCTION

Animal experimental burn models are essential to burn research because newly developed treatments must be evaluated in pre-clinical experiments prior to clinical use. An accurate study can only be achieved with burn-wound models that are of uniform size and depth. The degree of a burn injury is determined by the temperature, contact time and pressure of the heat source.[1] Although many burn models have been previously reported, most of the models involve the manual application of hot water or hot metal to the skin.[2-11] Although considerable efforts were made to maintain constant parameters, the manual creation of such burns is difficult to control and subject to human variability, particularly when performed by different operators. An automated method using a computer-controlled machine is therefore ideal for creating reproducible animal burn wounds.

We developed a new device which can automatically control the burn wound creation procedure to precisely maintain the critical factors associated with burn conditions, including the temperature, time and the pressure that is applied during the burning process. We inflicted burn wounds on the rat dorsum and attempted to explore the conditions that were appropriate for

preparing partial- and full-thickness burn wounds using this device. We evaluated the depth of the burn wounds under various conditions using laser speckle contrast imaging (LSCI), which is a modification of the widely accepted laser Doppler perfusion imaging (LDI) technique[12], which assesses the microvascular blood flow of burn wounds based on flux.[11,13,14] The healing process was also macroscopically and histologically observed until complete re-epithelialization for precise evaluation of the burn-wound depth.

The objective of this study was to evaluate the efficacy of a new burning device in preparing precise and reproducible animal burn models and to investigate the conditions that are required to prepare different depths of burn wounds using our new device.

MATERIALS AND METHODS

1. The specifications of the burning device

The characteristics of the newly manufactured burning device are presented in Fig. 1. K. Kawai (Kyoto University) and Wellmer Co., Ltd. (Osaka, Japan) jointly developed this device. It has a movable Teflon-treated copper stamp head which contacts the animal's skin. The stamp contains an

electronically-controlled heating element which maintains the user-selected temperature (Fig. 1B). The stamp head can be varied according to the size of the wound that is required. We created circular stamps of 1 cm and 2 cm in diameter and a 1 cm^2 square stamp (Fig. 1C). We used a circular stamp of 2 cm in diameter for the experiments of the present study.

The pressure that is exerted on the skin is determined by weights that are placed on the stamp. By changing these weights, the pressure can be adjusted from 67.1 g/cm^2 to 593.3 g/cm^2 (Fig. 1D). The temperature of the stamp (room temperature to 200°C) and contact time (0.1 s to 99.9 s) can be set with a digital control panel (Fig. 1E). The temperature of the stamp head is continuously monitored and displayed in real time.

During the burning process, an anaesthetized animal is laid under the stamp, and the stamp is pressed onto the animal's skin using the weight of the stamp. At the selected time, the stamp is automatically withdrawn by an air compressor. The temperature of the stamp surface and the movement of the stamp are computer-controlled. Thus, the temperature, time and pressure of the stamp can be set individually, repeatedly and precisely.

2. Animals and operations

The animals were maintained at the Institute of Laboratory Animals, Graduate School of Medicine, Kyoto University. The experimental protocol was approved by the Animal Research Committee of Kyoto University (Med Kyo 14161). The number of animals that were used in this study was kept to a minimum, and all possible efforts were made to reduce their suffering in accordance with the protocols established by the Animal Research Committee of Kyoto University.

3. Preparation of burn wounds on rats

Nine-week-old F344 male rats (CLEA Japan, Inc., Tokyo, Japan) of approximately 200 g in body weight were used for the present study. The animals were housed in individual cages, and were acclimatized in a constant temperature and humidity unit for one week prior to the start of the study. The rats had *ad libitum* access to regular chow and water. After an intraperitoneal injection of pentobarbital sodium (30 mg/kg) (Somnopentyl®, Kyoritsu Seiyaku Corporation, Tokyo, Japan), the entire dorsum of the animal was shaved and depilated using normal depilation cream. The animal

was placed under the stamp of the burning device, which was heated to the selected temperature and pressed onto the animal's skin at a constant pressure. This burning process was repeated on both sides, thus two wounds were prepared on the back of each animal.

In the experiments of the present study, the temperature of the stamp was set at 80°C and the weight was 110 g/cm^2, while the contact time was set at 2, 4 or 10 s. Each group included 9 rats with 18 experimental wounds: 2 rats (four wounds) in each group were used to observe wound healing; the other 7 rats (14 wounds) were used for the histological study.

Because of the difficulty in identifying the burn-wound margin in the rat burn model, the burn-wound margin after wounding was clarified by tattooing at eight points by pricking with 27G needles containing India ink. The burn wounds were covered with polyethylene film (Tegaderm®, 3M Health Care, St. Paul, MN, USA) to prevent them from drying. They were then wrapped with an elastic adhesive bandage tape (Silkytex®, Alcare Co., Ltd., Tokyo, Japan).

4. The evaluation of the burn wounds

4.1. The gross appearance and the burned area

Gross photographs of the four wounds in each group were taken at 1, 7, 14 and 24 days after wound creation under inhalation anesthesia with isoflurane (Wako Pure Chemical Industries Ltd, Osaka, Japan). The dressings were changed after the pictures were taken. The burned area marked by tattooing was independently determined by three plastic surgeons from photographs using an image processing software program (Image J ver. 1.45; NIH, Maryland, USA), and the mean area was used for the analysis.

4.2. Blood perfusion (flux) of the burned area

An FLPI (Moor Instruments, Devon, UK) (a laser speckle contrast imaging perfusion device), was used to measure the blood perfusion (flux) in all of the burn wounds on day 1 (n=18 in each group) under the inhalation of 1.5% v/v isoflurane. The evaluation was performed in a quiet environment at 24 ± 2°C just after the induction of anesthesia, before the body temperature decreased. Measurements were performed five times for each wound; the average flux value was used for the analysis.

4.3. The histological evaluation of burn wounds

Five rats in each group were sacrificed after the inhalation of carbon dioxide gas on day 1 and 1 rat in each group was sacrificed on days 7 and 14. Burn-wound tissue specimens were harvested with the surrounding intact skin. The excised tissues were fixed in 10% buffered formaldehyde solution for 24 h and embedded in paraffin wax. Axial sections of 6 μm in thickness were prepared.

4.3.1. The histological evaluation of the burn depth

Axial sections from the center of each specimen on day 1 (n=10: 10 wounds from 5 rats in each group) were prepared and stained with either haematoxylin and eosin (HE) or azocarmine and aniline blue (AZAN). The depths of the burn wounds were histologically evaluated using the HE- and AZAN-stained burn-wound sections. The injured area was detected (based on the methods of a previous study[15]) by observing collagen alteration (collagen hyalinization with a corresponding loss of individual collagen fiber distinction), vascular occlusion, follicular injury (the follicle epithelia exhibited features that were consistent with cellular injury) and muscle fiber

alteration. The perpendicular distance between the tissue surface and the burn interface with normal tissue was determined at three points (the left, center and right of each specimen) and the mean distance was calculated.

4.3.2. The epithelialization rate (ER) of burn wounds

We determined the ER on days 1, 7 and 14 to evaluate the epithelialization from the skin appendages. The ER was defined as the percentage of the length of epithelialized tissue in comparison to the wounds on HE-stained sections (Fig. 2). The ER was determined over an area of 4 mm in length at the center of each section, because the wound healing in this area was unaffected by the epithelialization from the marginal skin (Fig. 2A). Three axial sections were prepared from the central, 4 mm cranial and 4 mm caudal areas, and the ER was determined in these sections (Fig. 2B). The estimation was performed independently by three plastic surgeons who were blinded to the exposure duration. The mean values of their estimations were used for the analysis (n=6 in each group).

5. Statistical analysis

All data are descriptively expressed as the means ± standard deviation. P values of < 0.05 were considered to be statistically significant. Normality was tested using the chi-square goodness of fit test. The homogeneity of variance was tested using the Bartlett test. Multiple comparisons were performed by a one-way analysis of variance (ANOVA) with the Tukey Kramer multiple comparisons post-test, as the normality and the homogeneity of variance was confirmed in the burned area, blood perfusion and the burn wound depth in the histological samples. The Steel-Dwass test for multiple comparisons (a nonparametric procedure) was used to analyze the ER data, as they were not normally distributed and lacked homogeneity of variance.

RESULTS

1. The time course of the burn wounds

The gross appearances of the wounds in each group on days 1, 7, 14 and 24 are presented in Fig. 3. The surface of the burned skin became whitish in all groups immediately after preparation. Thicker necrotic tissue was observed in the 4s and 10s groups. Their surfaces were whiter than those of the 2s group on day 1. On day 7, dotted epithelialization from the remaining

intact dermis was first observed in the 2s group, while a small amount of necrotic tissue was observed on the wound surface in the 4s group and thicker necrotic tissue was found in the 10s group. On day 14, the epithelialization was mostly completed in the 2s group, and dotted epithelialization from the skin appendages was observed in the 4s group without severe wound contracture. In contrast, epithelialization from inside of the wound was not observed in the 10s group, and the wounds showed significant contracture. On day 24, the wounds in the 2s and 4s groups were completely epithelialized and displayed no severe contraction. In contrast, the wounds in the 10s group showed severe contraction, and epithelialization was incomplete.

The changes of the burned area over time indicated by the tattoo are presented in Fig. 4. The burned area in the 10s group was significantly smaller than the areas in the 2s and 4s groups on days 14 and 24 ($P<0.05$). This indicated that the wounds in the 10s group displayed significantly more contraction on days 14 and 24 in comparison to the 2s and 4s groups, whereas there was no significant difference in the contraction between the 2s and 4s groups ($n=4$).

2. Blood perfusion of the burned area

Color-coded images of the burn wound surface were generated using the FLPI on day 1 (Fig. 5). High perfusion areas are indicated by red and low perfusion by blue in the images. The mean flux values of the burn wound area on day 1 in the 2s, 4s and 10s groups were 548.8 ± 57.0, 364.3 ± 59.7 and 266.5 ± 46.5, respectively (Fig. 6). The flux value in the 4s group was significantly lower than that in the 2s group ($P<0.01$), and the flux value in the 10s group was significantly lower than that in both the 2s and 4s groups ($P<0.01$) ($n=18$).

3. The histological evaluation of burn wound depth

HE- and AZAN-staining micrographs of burn wounds in the 2s, 4s and 10s groups on day 1 are presented in Fig. 7. The burning process induced epidermis detachment in all of the groups. The dotted line indicates the interface of the heat-injured area according to the histological damage to the dermal collagen, capillaries, and hair follicles.

In the 2s group, the heat-affected area was restricted to only the superficial region of the dermis. In the 4s group, the deep part of the dermis was affected; only the hair follicles in the lower part of the dermis remained

intact. Part of the panniculus carnosus below the dermis was injured in the 10s group in addition to the entire dermis, whereas skeletal muscles in the deeper layer were undamaged by the heat energy.

Burn depth was assessed in the histological samples as the perpendicular distance between the tissue surface and the interface with normal tissue (Fig. 8). The burn depth was significantly deeper in the 4s group than in the 2s group ($P<0.01$), while the burn depth in the 10s group was deeper than that in the 2s and 4s groups ($P<0.01$) ($n=10$).

4. The evaluation of burn-wound epithelialization

Figure 9 shows micrographs of HE-stained burn wound sections in the 2s, 4s and 10s groups on days 1, 7 and 14. In the 2s group, epithelialization from the remaining hair follicles was observed on day 7, and epithelialization was completed by day 14. In the 4s group, epithelialization was not clearly observed on day 7, but it was mostly completed on day 14. In contrast, no epithelialization from the hair follicles was observed in the 10s group.

Figure 10 shows the time course of the ER. In the 2s and 4s groups, the ER increased with time. The ERs in the 2s group on day 7 ($P<0.05$) and

in the 2s and 4s groups on day 14 ($P<0.01$) were significantly higher than the ER in the 10s group (n=6).

DISCUSSION

A number of rat burn models and various modalities for setting burn wound parameters have so far been reported. In one study, a partial-thickness burn wound was prepared by exposing the dorsal surface of a rat to 95°C water for 2 seconds[4]. In another study, a full-thickness burn wound was prepared by pressing a stainless steel rod (heated with boiling water [100°C]) onto the skin for 10 seconds with 127g/cm^2 of contact pressure[9]. Referring to their settings, we used a temperature of 80°C and 110g/cm^2 of contact pressure and contact times of 2, 4 and 10 s to prepare burn wounds of varying thickness. The technique used in the present study differs from the above-mentioned manual procedures in two key aspects: we maintained the temperature of the stamp throughout the procedure, and we measured the contact time with 1/10 second accuracy.

Kistler et al.[1] reported the creation of an automated burning device to produce animal burn models; however, the aim of their report was to

investigate the pathophysiology of severe burn injuries. They produced only full-thickness burns and investigated general conditions such as the mortality rate. Kistler et al. paid no attention to the healing process of burn wounds and did not prepare partial-thickness burns. There are no other reports concerning the use of automated devices in the creation of animal burn models.

The novel automatic device of the present study is an improvement of Kistler's burning device. It is similar to Kistler's apparatus in that it can control the temperature, time and pressure. Our device offers improved usability through its digital control panel and microprocessor. The advantage of our model over most of the previously reported manual burn models is the decreased range of errors in the parameters that are used to determine the burn wound depth. The surface temperature of the stamp is continuously controlled within an error range of ± 2°C, and the contact time is strictly controlled within an error range of ± 0.05s by the microprocessor. The contact pressure is determined by the weight of the structure over the stamp.

We attempted to prepare superficial dermal burns (SDBs) and deep dermal burns (DDBs) using the precise settings of our novel device. The burn

wounds were evaluated on day 1 by a histological examination and a blood perfusion test using LSCI, and were observed until complete re-epithelialization. Due to the difficulties in measuring epithelialization using gross photographs, we used the epithelialization rate (which was measured in the histological burn wound sections) as a precise measurement of epithelialization. The presence of epithelialization from skin appendages is the diagnostic criterion of a partial-thickness burn.

In the present study, the flux value of the burn wounds, which was measured using an LSCI device, decreased according to the contact time. In a swine burn model that was evaluated by LSCI, the tissue perfusion of burn wounds was reported to decrease according to the depth of the wound.[7] The injured area was histologically limited to the superficial layer of the dermis in the 2s group. In contrast, the deeper layer of the dermis was injured in the 4s group, and wound healing was retarded in comparison to the 2 s group. In the 10s group, the whole dermis was damaged, and no epithelialization from the remaining epidermal cells was observed. In the 10s group, the wounds healed with contraction and epithelialization from the wound margins. These histological findings indicated that the depths of the burn wounds in the 2s,

4s and 10s groups corresponded with SDB, DDB and full-thickness burns, respectively.

This study confirmed that our new burning device can reproducibly create burn wounds of a desired depth. The burning device presented in this study is commercially available from Wellmer Co., Ltd., Osaka, Japan (information@wellmer-jp.com). Using this device, anyone can create the same burn wounds and animal burn models can be standardized.

Although the epidermis and dermis of rats are similar to human skin, the wound healing mechanisms of rats differ substantially from humans. Larger animals, such as pigs, may therefore be better for investigating the effectiveness of new drugs or wound dressings. Our next step is to use the device developed in the present study to generate burn wounds in larger animals.

Conclusion

Precise burn wounds can be produced on the skin of experimental animals using our new automated, computer-controlled burning device by adjusting the stamp size, temperature, pressure and contact time.

Conflict of interest

The authors declare no conflicts of interest in association with the present study.

Acknowledgements

This work was supported by the Japan Society for the Promotion of Science (JSPS)

KAKENHI Grant Number 24390399.

REFERENCES

1. Kistler D, Hafemann B, Schmidt K. A model to reproduce predictable full-thickness burns in an experimental animal. *Burns Incl Therm Inj* 1988;14(4):297-302
2. Singer AJ, Hirth D, McClain SA, et al. Validation of a vertical progression porcine burn model. *J Burn Care Res* 2011;32(6):638-46
3. Walker HL, Mason AD Jr. A standard animal burn. *J Trauma* 1968;8(6):1049-51
4. Yurt RW, McManus AT, Mason AD Jr, et al. Increased susceptibility to infection related to extent of burn injury. *Arch Surg* 1984;119(2):183-8
5. Abdullahi A, Amini-Nik S, Jeschke MG. Animal models in burn research. *Cell Mol Life Sci* 2014;71(17):3241-55
6. Kaufman T, Lusthaus SN, Sagher U, et al. Deep partial skin thickness burns: a reproducible animal model to study burn wound healing. *Burns* 1990;16(1):13-6
7. Ponticorvo A, Burmeister DM, Yang B, et al. Quantitative assessment of graded burn wounds in a porcine model using spatial frequency domain

imaging (SFDI) and laser speckle imaging (LSI). *Biomed Opt Express* 2014:5(10):3467-81

8. Kim DE, Phillips TM, Jeng JC, et al. Microvascular assessment of burn depth conversion during varying resuscitation conditions. *J Burn Care Rehabil* 2001;22(6):406-16

9. Cai EZ, Ang CH, Raju A, et al. Creation of consistent burn wounds: a rat model. *Arch Plast Surg*. 2014;41(4):317-24

10. Mitsunaga Junior JK, Gragnani A, Ramos ML, et al. Rat an experimental model for burns: a systematic review. *Acta Cir Bras* 2012 ;27(6):417-23

11. Khatib M, Jabir S, Fitzgerald O'Connor E, et al. A systematic review of the evolution of laser Doppler techniques in burn depth assessment. *Plast Surg Int 2014*. 2014:621792. doi: 10.1155/2014/621792. Epub 2014 Aug 7.

12. Qin J, Reif R, Zhi Z, et al. Hemodynamic and morphological vasculature response to a burn monitored using a combined dual-wavelength laser speckle and optical microangiography imaging system. *Biomed Opt Express* 2012;3(3):455-66

13. Kloppenberg FW, Beerthuizen GI, ten Duis HJ. Perfusion of burn wounds assessed by laser Doppler imaging is related to burn depth and healing

time. *Burns* 2001;27(4):359-63

14. Droog EJ, Steenbergen W, Sjöberg F. Measurement of depth of burns by laser Doppler perfusion imaging. *Burns* 2001;27(6):561-8.

15. Meyerholz DK, Piester TL, Sokolich JC, et al. Morphological parameters for assessment of burn severity in an acute burn injury rat model. *Int J Exp Pathol* 2009;90(1):26-33

Figure legends

Fig. 1. The characteristics of the burning device.

(A) The black arrow indicates the stamp head which contacts the skin. Magnified image: (B). The white arrow indicates the weights that are used to adjust the pressure. Magnified image: (D). The arrow head indicates the control panel, which is used to set the temperature and contact time. Magnified image: (E). (C) The different stamp heads: a round head of 1 cm in diameter (left), a 1 cm^2 square head (center) and a round head of 2 cm in diameter (right).

Fig. 2. The evaluation of the epithelialization rate (ER)

(A) A macroscopic view of the burn wounds on day 14 in the 4s group. Three histological sections from the center and areas 4 mm cranial and caudal from the center, are indicated by black lines. The ER was evaluated in the central part (4 mm in length), which is indicated by black boxes in each section.

(B) The evaluation of the ER in HE-stained burn wound sections on day 14 in the 4s group. The ER was equal to the length of the epithelialized tissue (b) divided by the wound length (4mm) (a).

Fig. 3. The gross appearance of the burn wounds.

The wound margin was tattooed at eight points.

Fig. 4. The time course of the changes in the burned area.

The burned area in the 10s group was significantly smaller than the burned areas of the 2s and 4s groups on days 14 and 24 (n=4).

*P<0.05 vs. the 10s group. **P<0.01 vs. the 10s group.

Fig. 5. Color-coded images generated by FLPI

Color-coded maps of the 2s (A), 4s (B) and 10s (C) groups on day 1. Red indicates high blood flow. Blue indicates low blood flow. The tattoo could be confirmed on these images. The wound in the 2s group was red or green, while that in the 10s group was dark blue.

Fig. 6. The flux values

The comparison of the flux values in the 2s, 4s and 10s groups on day 1. The flux value in the 4s group was significantly lower than that in the 2s group.

The flux value in the 10s group was significantly lower than the values in the 2s and 4s groups (n=18). **P<0.01.

Fig. 7. The results of the histological evaluation of the burn wound depth in micrographs of HE-stained (upper) and AZAN-stained (lower) burn wound sections from the 2s, 4s and 10s groups on day 1. The dotted line indicates the border of the heat-injured dermis. Yellow arrows indicate denatured hair follicles. Red arrows indicate coagulated vessels. Black arrow heads indicate the damaged panniculus carnosus. The superficial part of the dermis in the 2s group and the deeper part of the dermis in the 4s group were damaged. The entire dermis and panniculus carnosus were damaged in the 10s group.

Fig. 8. The histological evaluation of burn depth in HE-stained burn wound sections

The burn wound depth in the 4s group was significantly larger than that in the 2s group, while the burn wound depth in the 10s group was larger than that in the 2s and 4s groups (n=10). **P<0.01.

Fig. 9. The histological evaluation of epithelialization in HE-stained burn wound sections.

Micrographs of HE-stained burn wound sections from the 2s, 4s and 10s groups on days 1, 7 and 14. The black arrows indicate epithelialized tissue.

Fig. 10. The time course of the changes in the ER

The ER in the 2s, 4s and 10s groups on days 1, 7 and 14. The ER increased with time in the 2s and 4s groups. No epithelialization was observed in the 10s group (n=6).

* $P<0.05$ vs. the 10s group, ** $P<0.01$ vs. the 10s group.

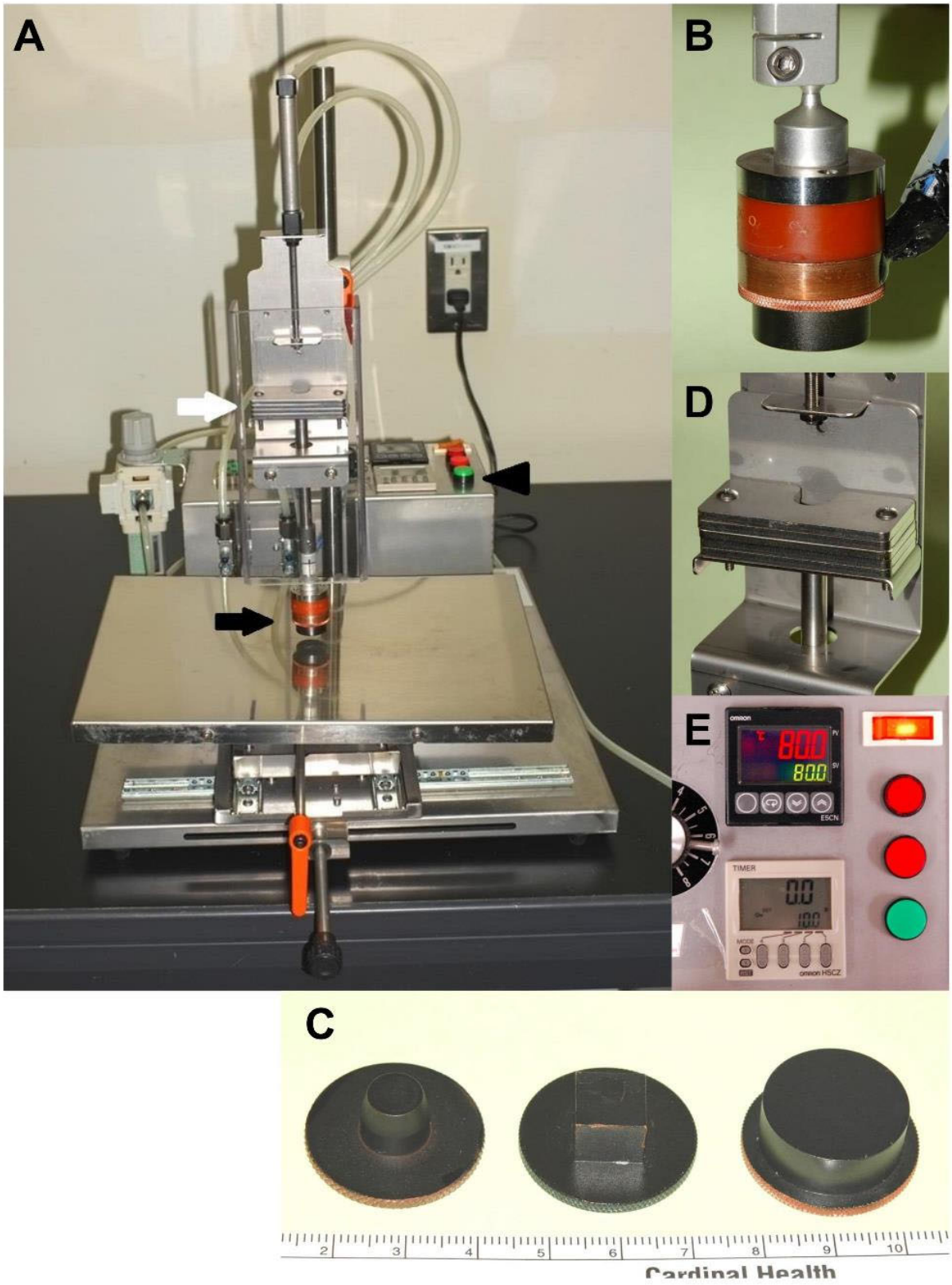

Fig.1.

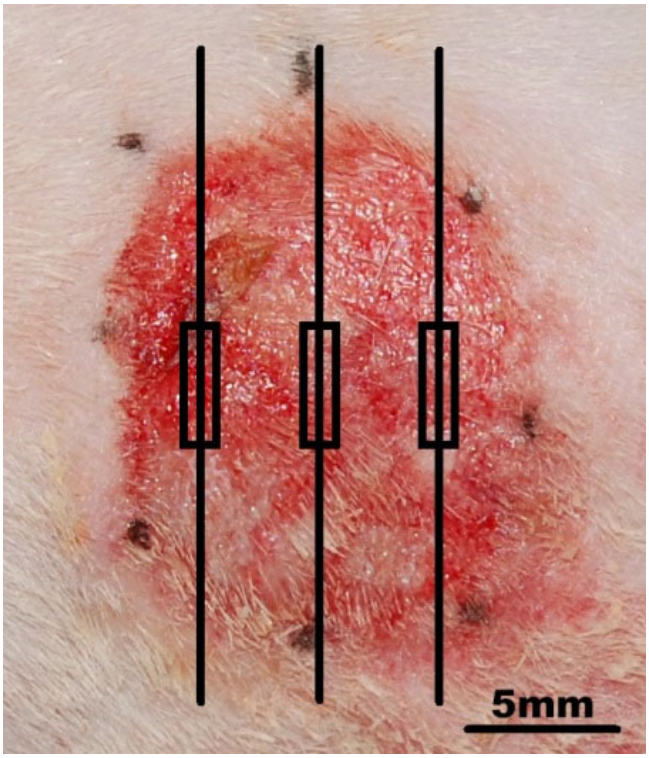

Fig.2A.

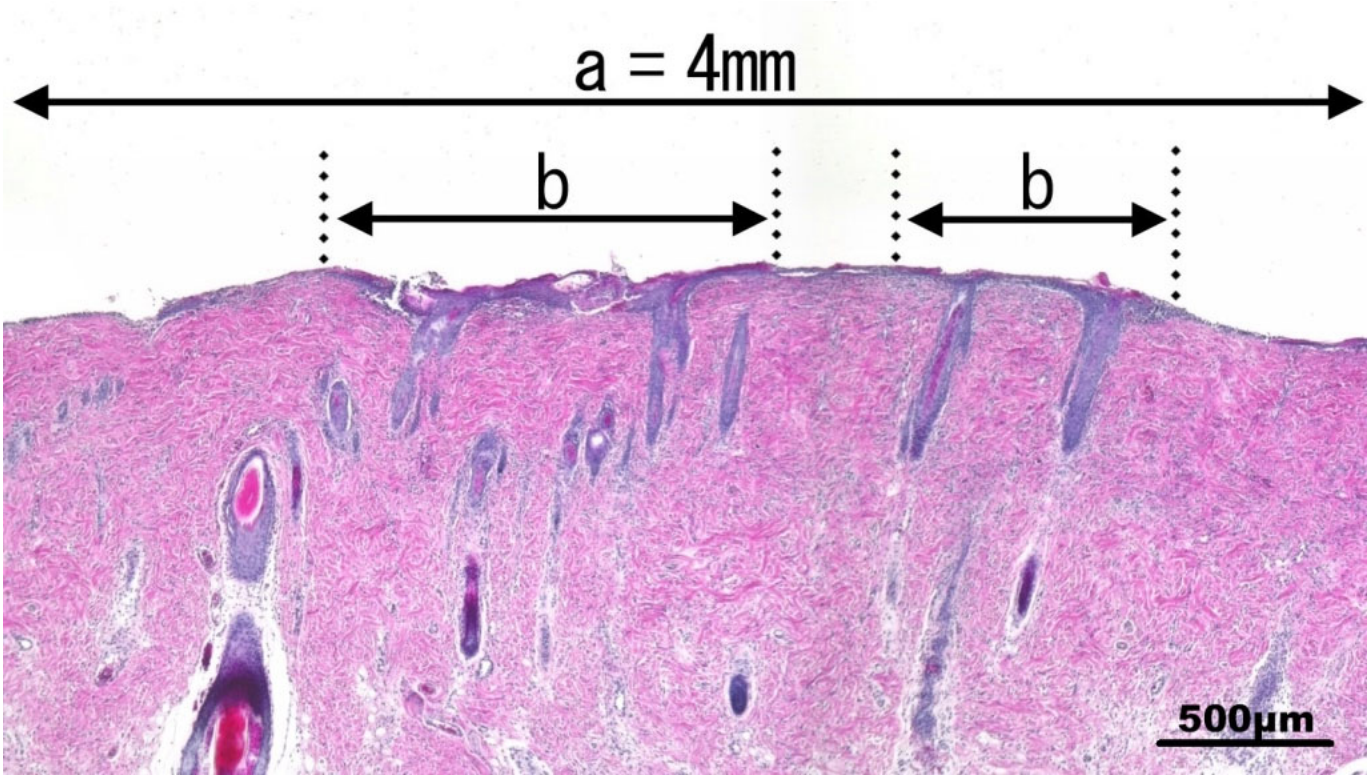

Fig.2B.

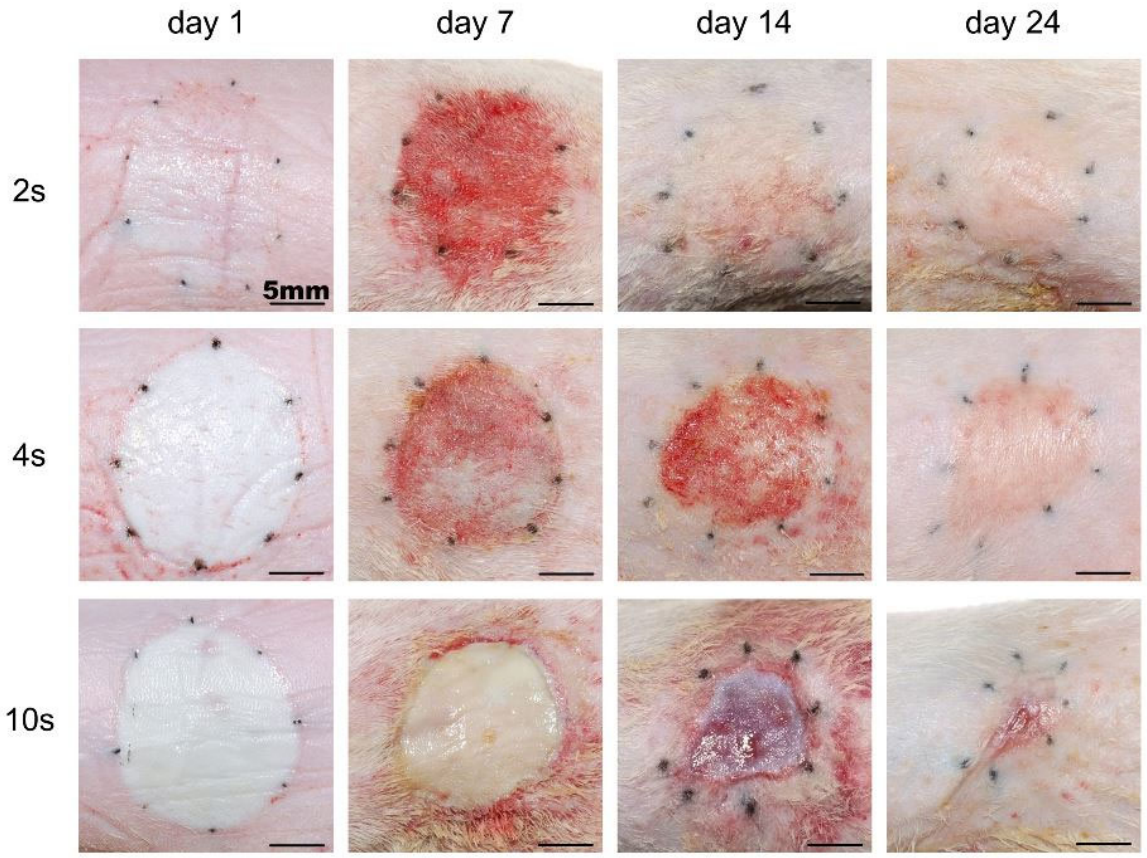

Fig.3.

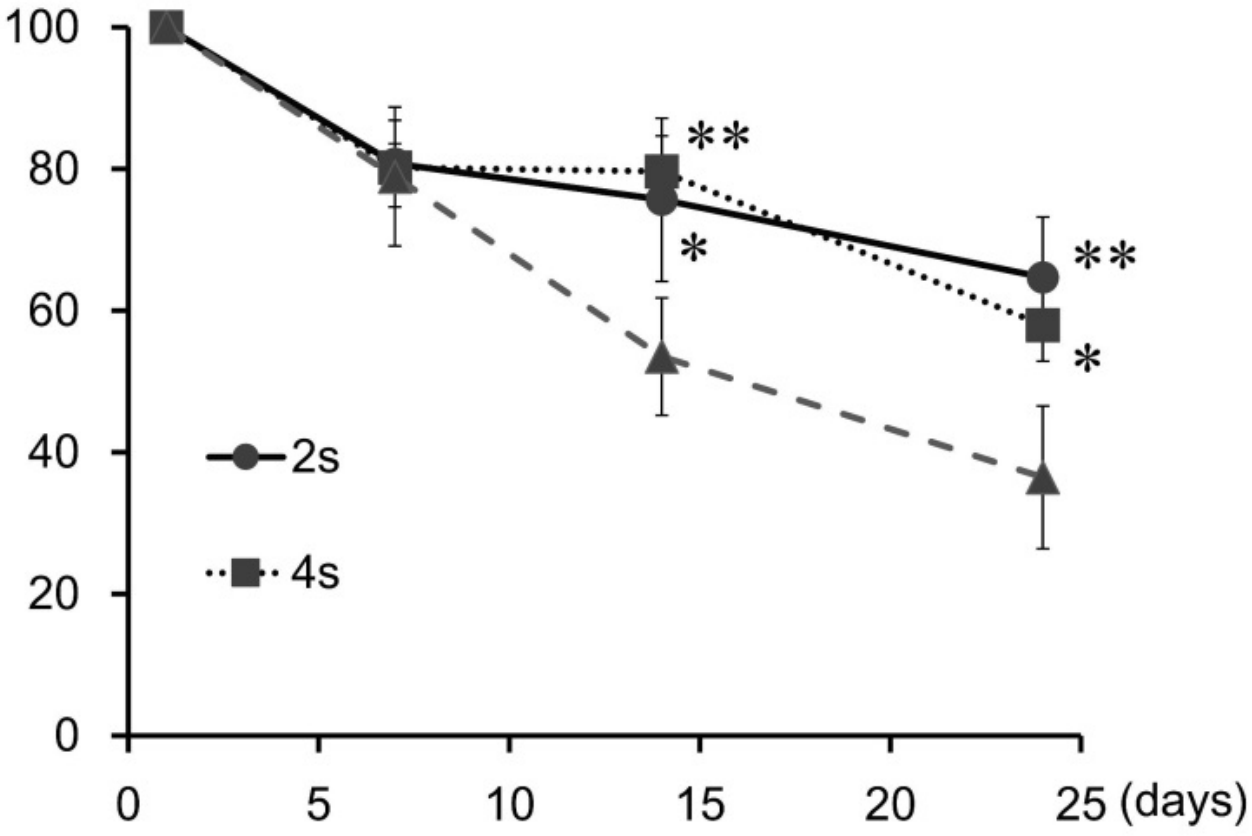

Fig.4.

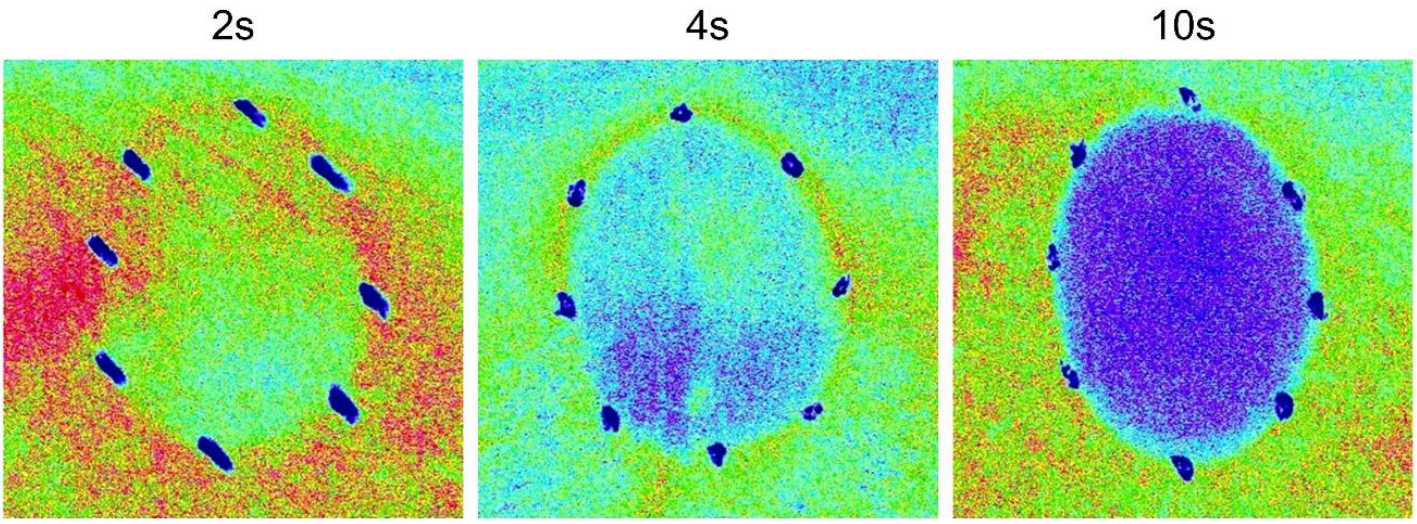

Fig.5.

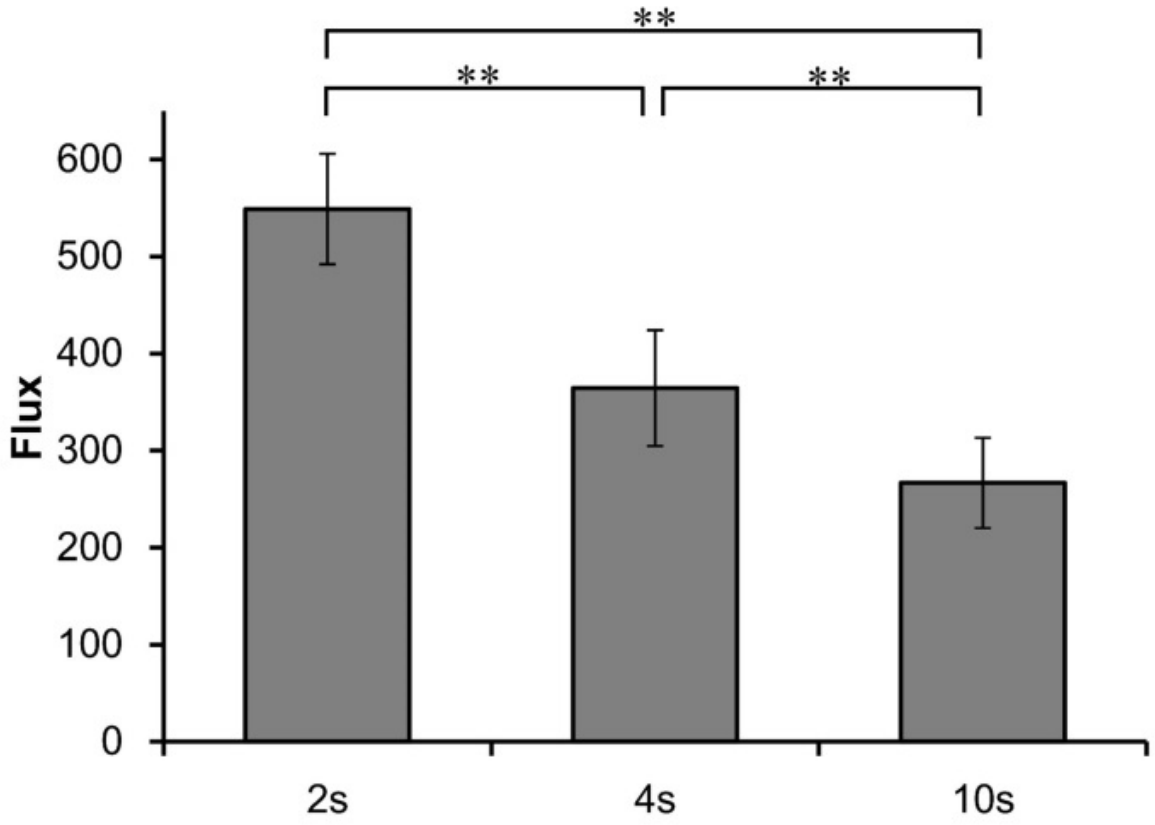

Fig.6.

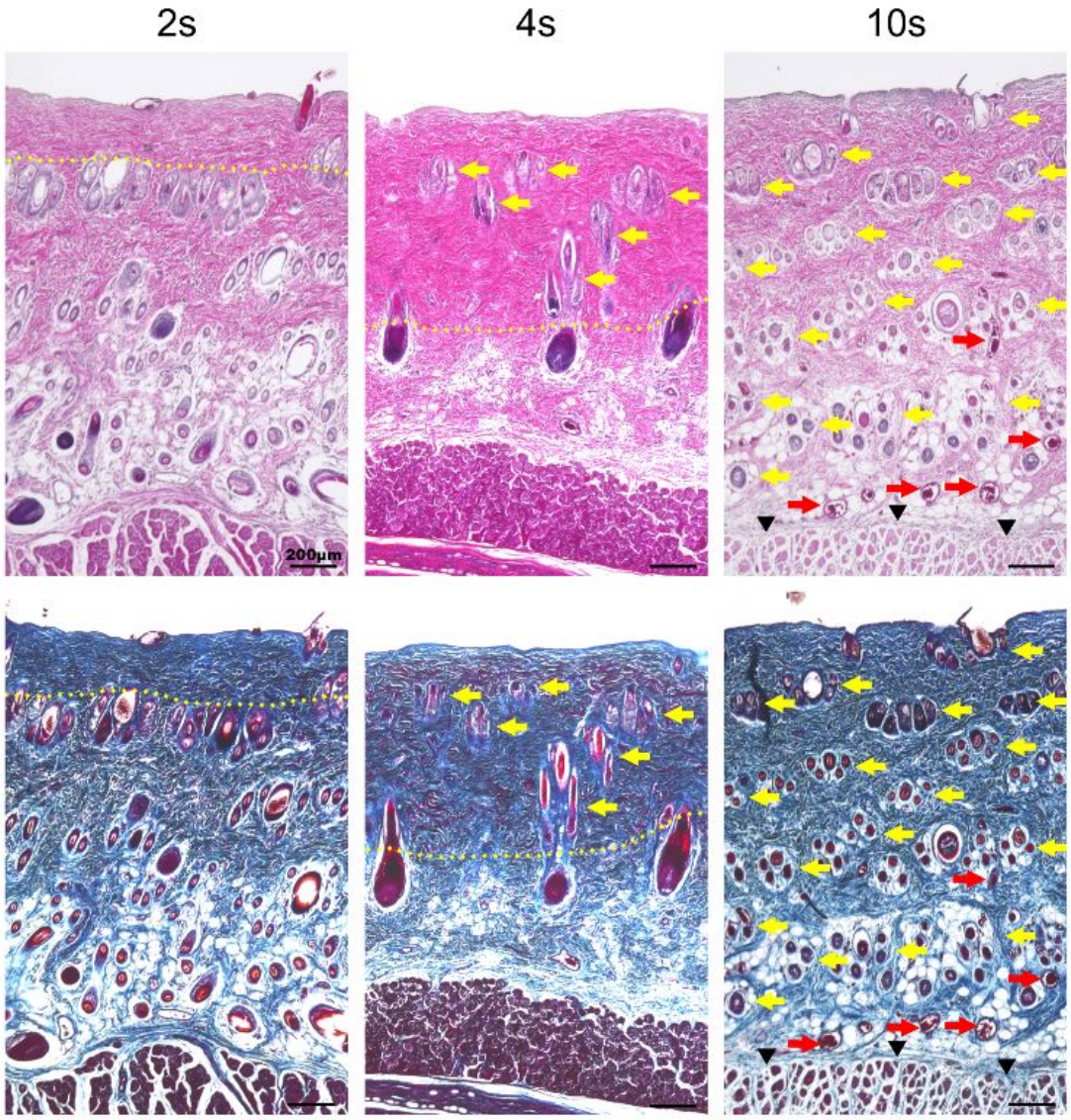

Fig.7.

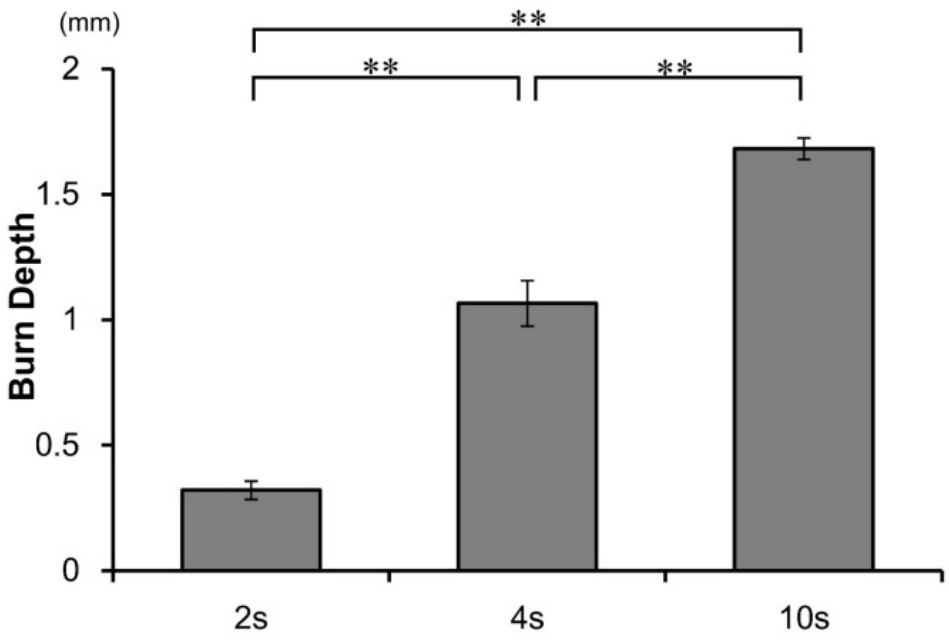

Fig.8.

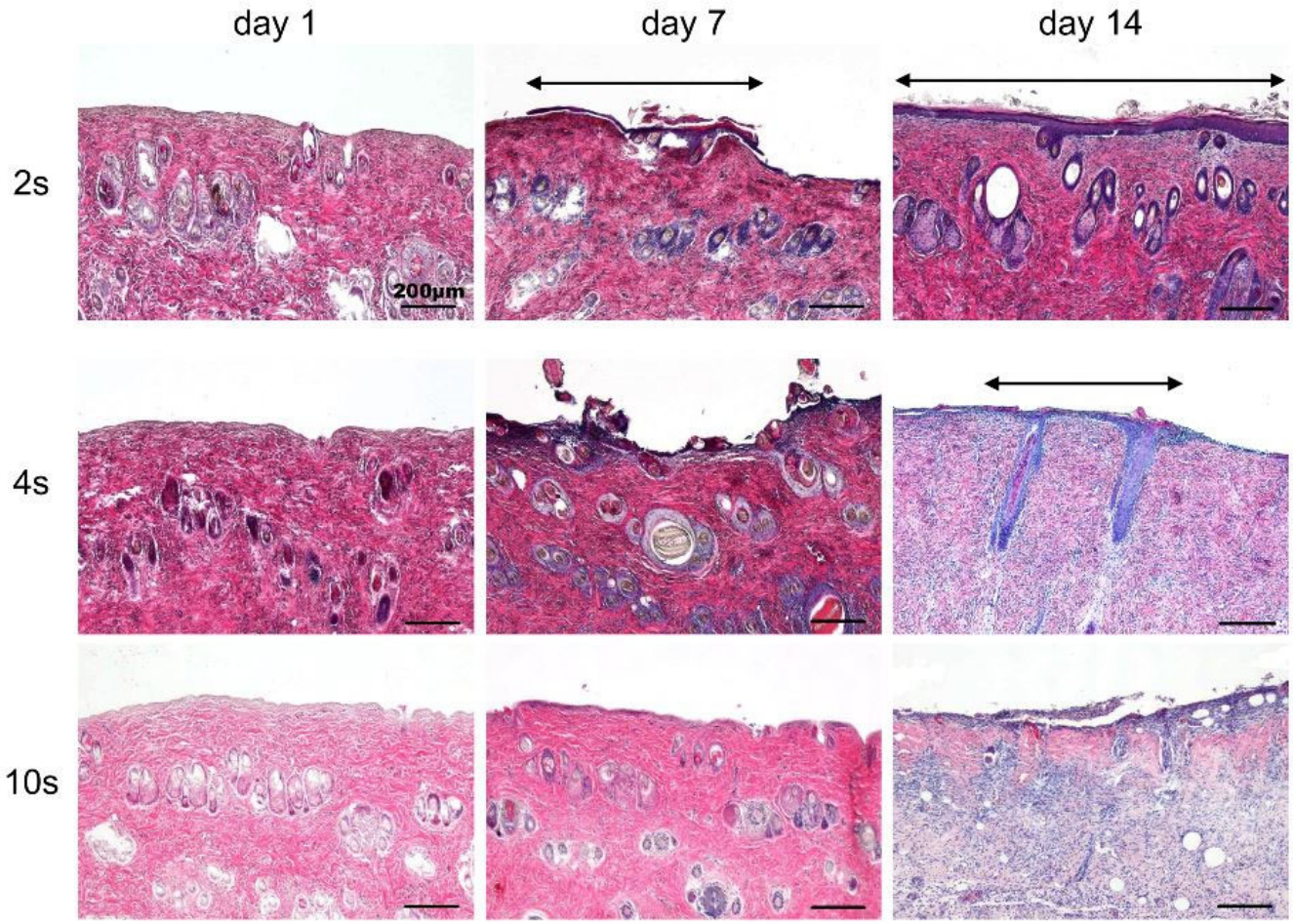

Fig.9.

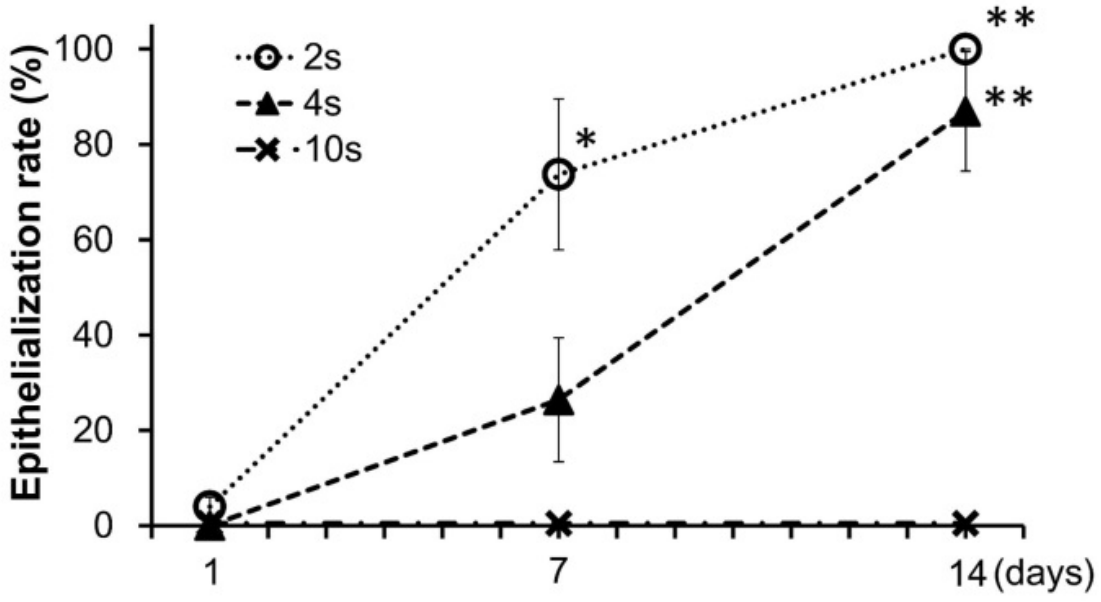

Fig.10.